Available online at www.sciencedirect.com
ScienceDirect
International Journal of Pharmaceutics 341 (2007) 195–206
INTERNATIONAL JOURNAL OF PHARMACEUTICS
www.elsevier.com/locate/ijpharm

Pharmaceutical Nanotechnology

Drug release study of large hollow nanoparticulate aggregates carrier particles for pulmonary delivery

Kunn Hadinoto [a,*], Kewu Zhu [a], Reginald B.H. Tan [a,b]

[a] *A*STAR Institute of Chemical and Engineering Sciences, Singapore 627833, Singapore*
[b] *Department of Chemical & Biomolecular Engineering, National University of Singapore, Singapore 119260, Singapore*

Received 13 December 2006; received in revised form 10 March 2007; accepted 24 March 2007
Available online 30 March 2007

Abstract

The aim of the present work is to examine the viability of using large hollow nanoparticulate aggregates as the therapeutic carrier particles in dry powder inhaler delivery of nanoparticulate drugs. The large hollow carrier particles are manufactured by spray drying of nanoparticulate suspensions of biocompatible acrylic polymer with loaded drugs. The size and concentration of the nanoparticles, as well as the phospholipids inclusion, have been known to influence the resulting morphology (i.e. size and degree of hollowness) of the spray-dried carrier particles. The effects of the resulting morphology of the carrier particles on the drug release rate are therefore investigated by varying the above three variables. The results of the drug release study are presented using aspirin and salbutamol sulfate as the model drugs with a varying degree of water solubility. The results indicate that the drug release rate is governed by the degree of hollowness of the carrier particles, and to a lesser extent by the nanoparticles size, as a result of the variation in the drug loading capacity of nanoparticles of different sizes.

Keywords: Dry powder inhaler; Pulmonary delivery; Hollow particles; Nanoparticulate drugs; Drug release; Formulation

1. Introduction

Dry powder inhaler (DPI) delivery of therapeutic agents has recently become a subject of very active research with the FDA approval of the use of spray-dried insulin dry powder aerosols, Exubera from Pfizer, to treat patients with type 1 and type 2 diabetes. The FDA approval of Exubera provides a major boost for research activities in discovering innovative pharmaceutical technologies to deliver therapeutic agents by inhalation for systemic circulation. In pulmonary drug delivery, the inhaled particles are subjected to the phagocytic clearance mechanism in the lung alveolar region by the scavenging alveolar macrophages. The lung phagocytosis is most significant for particles having geometric diameter (d_g) between 1 and 2 μm, and diminishes for particles having smaller or larger geometric diameters (Ahsan et al., 2002; Makino et al., 2003). Recent studies on pulmonary nanoparticle deposition suggest that inhaled nanoparticles (<100 nm) are the optimal particle size for alveolar deposition, as well as for minimizing the lung phagocytosis (Hoet et al., 2004).

However, the application of nanoparticulate drugs for DPI delivery is not straightforward, as direct inhalation of nanoparticulate drugs is not feasible due to their extremely small size. The nanometer size leads to the nanoparticulate drugs being predominantly exhaled from the lungs, without any deposition taking place. Moreover, a severe aggregation problem arising from the small size makes their physical handling extremely difficult for DPI delivery. To circumvent the above problems, a novel formulation technique to manufacture large hollow carrier particles of nanoparticulate drugs has been developed by Tsapis et al. (2002) using a spray drying technique. The formulation technique has since been subsequently enhanced by Hadinoto et al. (2006).

The large and hollow features of the carrier particles are specifically designed to produce inhaled particles with high aerosolization efficiency and high therapeutic efficacy (Edwards et al., 1997). The large hollow carrier particles, whose shells are composed of nanoparticulate aggregates, exhibit a large geometric diameter ($d_g \approx 10$–15 μm), but with a small aerodynamic diameter ($1 \leq d_a \leq 3$ μm). The small aerodynamic diameter of

* Corresponding author. Tel.: +65 6796 3858; fax: +65 6316 6183.
E-mail address: kunn.hadinoto@gmail.com (K. Hadinoto).

0378-5173/$ – see front matter © 2007 Elsevier B.V. All rights reserved.
doi:10.1016/j.ijpharm.2007.03.035

Nomenclature

D.O.F.	the degree of freedom
$n_{1,2}$	the number of independent replicates of samples 1 and 2
$s_{1,2}$	the standard deviation of samples 1 and 2
$x_{1,2}$	the mean of samples 1 and 2

Greek letters

α	the probability of error, alpha parameter, in the *t*-test
$\mu_{1,2}$	the mean of populations 1 and 2

the large hollow particles, which makes them highly suitable for DPI applications, is attributed to the hollow structure. Importantly, the nanoparticulate aggregates have been shown to disassociate into primary nanoparticles once they are exposed to an aqueous environment, such as in the alveolar lung region. Because the large hollow nanoparticulate aggregates re-disperse into nanoparticles having a much smaller size, they do not retain the shortcomings of the original large hollow particles developed by Edwards et al. (1997). Their large hollow particles have been shown to exhibit (1) an extremely slow drug release rate (particularly for water-insoluble drugs), and (2) a slow polymer degradation rate in the case of biodegradable polymers, which are both due to their large geometric size (Dailey et al., 2003).

In the present work, large hollow nanoparticulate aggregates of biocompatible PMMA-MeOPEGMa polymer nanoparticles with loaded drug have been manufactured. Salbutamol sulfate is used as the model for freely water-soluble drug (275 mg/mL at 20 °C), and aspirin is used as the model for lowly water-soluble drug (4.6 mg/mL at 20 °C). Salbutamol sulfate and aspirin have been chosen as the model drugs, because they are widely available and cost-effective. PMMA nanoparticulate-system has been chosen as the model nanoparticles due to its biocompatibility (Tao et al., 2003; Tapolsky et al., 2005), its high mechanical strength, and rigid polymeric structure (Stanek et al., 2006). The high structural-strength of the PMMA nanoparticles makes them highly suitable for use in the spray drying formulation, where a high-impact shear force is exerted on the nanoparticles by the atomizing fluid.

The details of the novel formulation technique have been presented in Hadinoto et al. (2006, 2007), and not repeated here. Briefly, nanoparticulate suspension containing the drug is spray-dried at a fast convective drying rate to ensure the formation of spherical nanoparticulate aggregates with large and hollow structures. A minimum threshold value in the concentration of the nanoparticulate suspension must be exceeded to obtain large hollow particles from the spray drying process. The effects of the chemical nature, size, and concentration of the nanoparticles on the resulting morphology of the carrier particles have been thoroughly investigated.

The goal of the present work is to examine the viability of using the large hollow nanoparticulate aggregates, which feature high aerosolization efficiency and high therapeutic efficacy, as the therapeutic carrier particles in inhaled delivery of nanoparticulate drugs. In that regard, an in vitro drug release study of the drug-loaded carrier particles in a phosphate buffer solution has been conducted. The authors are fully aware that, with regard to the aspirin, the nanoparticulate polymer delivery method is not the most suitable method of delivery due to the high dosage requirement of aspirin (~300 mg/day, compared to 400 μg/day for salbutamol sulfate). Therefore, the authors would like to emphasize that the aim of the present work is not to attempt to develop an improved method of delivering the aforementioned drugs, but rather to identify the key facets in the formulation of the large hollow nanoparticulate aggregates, which have significant impacts on the release rate of the therapeutic agents.

Specifically, the objective of the present work is to investigate the effects of (1) the nanoparticles size, and its spray drying concentration and (2) the inclusion of phospholipids (i.e. a major component of pulmonary surfactant) on the drug release rate. Our previous studies (Hadinoto et al., 2006, 2007) have shown the significance of the roles of the above three variables on the resulting morphology (i.e. size and degree of hollowness) of the large hollow nanoparticulate aggregates. Nonetheless, how they subsequently affect the release of drug from the nanoparticulate aggregates is not known. Therefore, the results of our study provide a comprehensive insight into the formulation of the large hollow nanoparticulate aggregates with loaded drug.

2. Materials and methods

2.1. Materials

The monomers for the synthesis of the polyacrylate nanoparticles, i.e. methyl methacrylate (MMa, purity ≥99%), methoxy(polyethylene glycol)methacrylate (MeOPEGMa, MW = 2000), and the initiator 4,4-azobis(4-cyanovaleric acid) (carboxy ADIB, purity ≥75+%) are purchased from Sigma–Aldrich, except for the MeOPEGMa, which is kindly supplied by Cognis Performance Chemicals (UK). Phospholipids S100 (95% phosphatidylcholine from fat free soybean lecithin) is purchased from Lipoid GmbH (Germany). Phosphate buffer solution in water (pH 7.2), TWEEN 20 surfactant, salbutamol sulfate and aspirin are purchased from Sigma–Aldrich. Ultra-pure water, hydrochloric acid, ethanol, ethyl acetate, acetonitrile and tetrahydrofuran analytical grade are used in the experiments.

2.2. Methods

2.2.1. Preparation and characterization of the PMMA-MeOPEGMa nanoparticles

PMMA-MeOPEGMa is prepared by a solution polymerization of MeOPEGMa and MMa in the proportions 15/85 (wt.%) as described in Phanapavudhikul et al. (2002). Ethyl acetate and ethanol are used as the solvents. The polymer is converted into polymer nanoparticles by a solvent replacement (also known as nanoprecipitation) technique. The nanoparticles exhibit steric colloidal stability arising from the MeOPEGMa component. Briefly, 0.15 g carboxy ADIB is dissolved in 15 mL ethanol and

55 mL ethyl acetate is added. The solution is refluxed for 45 min at 90 °C in a water-cooled reflux condenser. Separately, the feed solution is prepared by dissolving 0.13 g carboxy ADIB in 6 mL ethanol and 12.7 g MeOPEGMa is added. Next, MMa is poured according to its weight fraction in a separate beaker. The volume of both feed solutions is made up to 50 mL by adding ethanol. The two feed solution are added drop-wise into the solution that has been refluxed for 45 min, and let the polymerization run for about 2 h at 90 °C.

At the end of the polymerization, the temperature is maintained at 90 °C to partially evaporate the ethyl acetate, while 50–100 mL ethanol is continuously added to prevent the polymer from drying out. The drug-loaded nanoparticles are prepared by dissolving a certain amount of drug in the 50–100 mL ethanol. Next, the solvent is displaced by adding water drop-wise at 70 °C inducing a macromolecular rearrangement of the polymer to form colloidally stable particles, which is evident as the solution gradually becomes cloudy in its appearance. Continue heating at 70 °C to let the remaining ethanol evaporate. A wide range of nanoparticles sizes can be obtained by varying the amount of ethanol added after the polymerization steps. The size of the nanoparticles is measured by dynamic light scattering, also known as photon correlation spectroscopy, using Zetasizer Nano-ZS (Malvern, UK).

2.2.2. Preparation and characterization of the large hollow carrier particles

B-290 Mini Spray Dryer (Büchi, Switzerland), which operates on the principal of a two-fluid atomizer, is employed in the spray drying of nanoparticulate suspension to produce the large hollow nanoparticulate aggregates. The following spray drying operating condition is employed: inlet temperature of 105 °C, compressed air flow rate of 250 L/h, and feed rate of 4.0 mL/min. The resulting outlet temperature at the above operating condition is approximately 60 °C. In the sample preparation of the spray-dried particles for characterizations, the particles are stored in a desiccator for a 48-h period prior to the analysis. The geometric (d_g) and aerodynamic (d_a) diameters of the spray-dried particles are determined by light diffraction using particle size analyzer MS2000 (Malvern, UK) and time-of-flight measurement using particle size distribution analyzer PSDA 3603 (TSI, USA), respectively. The morphology of the spray-dried particles is examined using a scanning electron microscope (SEM) model JSM-6700F (JEOL, USA).

2.2.3. Determination of drug loading and drug entrapment efficiency

The percentage amount of the drug encapsulated per unit mass of the nanoparticles (i.e. the drug loading) is determined by dissolving 50 mg of the freeze-dried polymer nanoparticles in 10 mL acetonitrile. The resulting solution is next analyzed using a UV–vis spectroscopy method (Shimadzu, Japan) at a wavelength of 277 nm for both aspirin and salbutamol sulfate. The drug entrapment efficiency is defined as the ratio of the mass of drug recovered in the nanoparticles to the initial mass of drug used in the formulation. The entrapment efficiency can be straightforwardly calculated, once the values of the drug loading and the concentration of the nanoparticles in the suspension are known. The suspension concentration (w/v) is determined by freeze drying (Freeze-dryer Alpha 1-4, Christ, Germany) 10 mL of the nanoparticulate suspension.

2.2.4. In vitro drug release and polymer degradation study

The in vitro drug release study is conducted using a dialysis bag (cellulose membrane, MW cut-off 12,400, Sigma–Aldrich), which (1) allows free diffusion of the drug molecules into the release medium, while at the same time (2) completely separates the nanoparticles from the release medium (Soppimath et al., 2001). The release study is conducted for the freeze-dried nanoparticles, the spray-dried large hollow carrier particles, and the free form of the drugs. About 400 mg of the drug-loaded particles are suspended in 10 mL of phosphate buffer solution (pH 6.8) inside a dialysis bag. The pH of the buffer solution is adjusted to 6.8 following the work of Torrado et al. (1996), and Guo et al. (2005) on aspirin release study. The pH is adjusted by mixing the original buffer solution with 1.0N HCl (2:1, v/v). Surfactant TWEEN 20 (0.5%, w/v) is added as a stabilizer. The dialysis bag is next placed in 115 mL of the buffer solution (sink condition) at 37 °C under magnetic stirring. At successive time intervals, aliquots (5 mL) of the release medium is collected and replaced with a fresh buffer solution. The collected sample is next analyzed using the UV–vis spectroscopy at 296 and 277 nm for the aspirin and salbutamol sulfate, respectively. Each experiment is conducted in triplicate.

The results of the release study conducted using the dialysis bag diffusion technique have been compared with a method without a dialysis bag, where the aliquots of the nanoparticulate suspension are centrifuged using an ultracentrifugation technique at 70,000 rpm for 60 min (Ultracentrifuge CP70MX, Hitachi, Japan). The results of the UV–vis spectroscopy of the two techniques do not indicate a significant variation in the UV–vis absorbance values (<5%), which indicates that the diffusion of the drug molecules through the dialysis membrane is more rapid than the drug release from the particles. Lastly, the molecular weight of the fresh polymer nanoparticles, and after 24 h immersion in the release medium, is determined using a gel permeation chromatography (GPC) technique (GPC 717, Waters, USA). The samples are freeze-dried and dissolved in tetrahydrofuran (THF). The GPC column is maintained at 40 °C with an injection flow rate of 0.3 mL/min.

2.2.5. Test of statistical significance

The statistical significance of the relationships among the data from different experimental groups is evaluated using the *t*-test statistical method. The goal of the statistical analysis is to determine whether the trends in the drug release profiles as a function of the nanoparticle size and phospholipids concentration are statistically significant, or due to a random occurrence. The details of the *t*-test analysis are presented in Appendix A.

3. Results

A summary of the experimental data is presented in Tables 1 and 2. The nomenclature NP represents the freeze-dried

Table 1
A summary of the experimental data: effects of the nanoparticles size

Description	NP size (nm)	NP recovery (mg/10 mL suspension)	Initial drug inclusion (g)	Drug entrapment efficiency (%)	Drug loading (%)	Spray-dried conc. (% w/w)	7-h Release (%)	24-h Release (%)
Freeze-dried NP	50 ± 20[a]	660	1.8	46	5.0	–	75	75
		460	1.8	19[b]	3.0	–	88	88
	70 ± 30[a]	550	0.9	31	2.0	–	88	88
	120 ± 40[a]	450	1.8	56	9.0	–	56	95
	170 ± 80[c]	250	0.2	63	2.0	–	65	80
	220 ± 100[a]	800	2.4	83	10.0	–	60	95
Spray-dried LHP w/o phospholipids	50 ± 20[a]	660	1.8	32	3.5	2.3	77	93
		460	1.8	16	2.5	1.6	81	93
	70 ± 30[a]	550	0.9	23	1.5	1.9	95	95
	120 ± 40[a]	450	1.8	56	9.0	1.4	58	94
	170 ± 80[c]	250	0.2	50	1.6	1.0	73	87
	220 ± 100[a]	800	2.4	83	10.0	2.3	54	81

[a] Aspirin-loaded.
[b] Dialyzed for 24 h to remove excess solvent.
[c] Salbutamol sulfate-loaded.

primary nanoparticles, whereas the nomenclature LHP represents the spray-dried large hollow nanoparticulate aggregates particles, whose shells are composed of the primary nanoparticles (NP).

3.1. Morphology of the large hollow nanoparticulate aggregates

SEM images of the spray-dried large hollow nanoparticulate aggregates, with loaded drugs, are presented in Fig. 1 (aspirin-loaded) and Fig. 2 (salbutamol sulfate-loaded). The SEM images show that a mixture of spherical large hollow particles (d_g = 10–15 μm) and very fine particles ($d_g \leq 3$ μm) is produced. The hollowness of the spray-dried particles is evident in their lower d_a values (≈3 μm) compared to their d_g values. A closer look at the surface of the large hollow particles, without loaded drug, reveals the nanoparticulate aggregates that compose the surface (see Fig. 3). A comprehensive discussion on the morphology of the large hollow nanoparticulate aggregates has been presented in Hadinoto et al. (2006, 2007).

The solid-state of the drug in the nanoparticles is determined by conducting a powder X-ray diffraction (PXRD, Bruker, UK) analysis, where the results indicate a completely amorphous state of the drug and the polymer nanoparticles. In other words, the drug is not present in its crystalline state, but rather it is either molecularly dispersed or physically dispersed in its amorphous

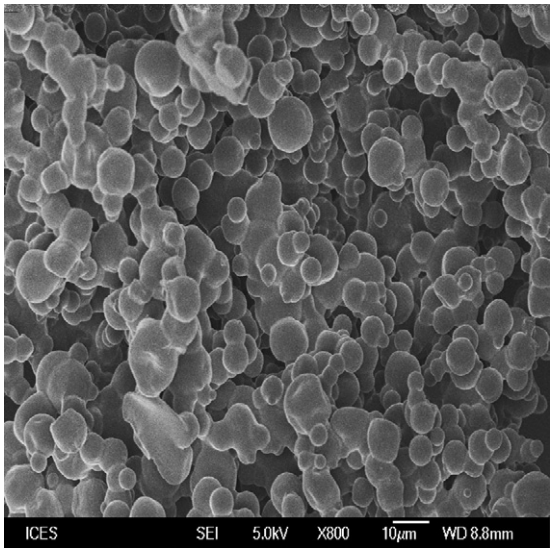

Fig. 1. Aspirin-loaded LHP of the 220 ± 100 nm NP spray-dried at 2.3% (w/w).

Table 2
A summary of the experimental data: effects of the phospholipids concentration

Description	NP size (nm)	NP recovery (mg/10 mL suspension)	Initial drug inclusion (g)	Drug entrapment efficiency (%)	Drug loading (%)	Spray-dried conc. (% w/w)	Phospholipids (% of total solids)	7-h Release (%)	24-h Release (%)
Spray-dried LHP w/o phospholipids	120 ± 40[a]	450	1.8	56	9.0	1.8	27	79	79
	170 ± 80[b]	250	0.2	50	1.6	1.2	20	68	68
						1.5	33	61	61
						2.6	9	50	77
	220 ± 100[a]	800	2.4	83	10.0	2.8	17	48	72
						3.1	24	50	65

[a] Aspirin-loaded.
[b] Salbutamol sulfate-loaded.

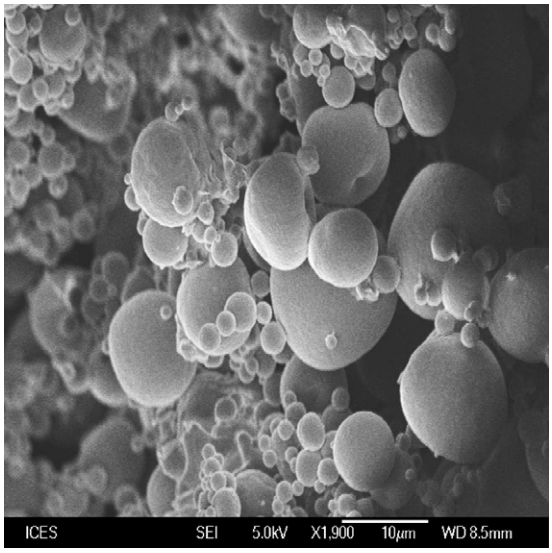

Fig. 2. Salbutamol sulfate-loaded LHP of the 170 ± 80 nm NP spray-dried at 1.0% (w/w).

state within the polymer matrix and/or on the nanoparticles surface (Sanchez et al., 1993).

3.2. Drug release rate as a function of the nanoparticles size

3.2.1. Different nanoparticles size, different drug loading

Aspirin-loaded nanoparticles having a wide range of sizes (i.e. 50 ± 20, 70 ± 30, 120 ± 40, and 220 ± 100 nm) are produced by varying the amount of ethanol (50–100 mL) added after the polymerization step. For the same initial amount of drug used (1.8 g), the variation in the nanoparticles size leads to a variation in the drug loading and drug entrapment efficiency of the nanoparticles, where larger size nanoparticles exhibit larger values for both (see Table 1). The results also indicate that the values of the drug loading and drug entrapment efficiency of the smaller size nanoparticles (i.e. 50 ± 20 and 70 ± 30 nm) slightly decrease after spray drying, which is not observed for the larger size nanoparticles (120 ± 40 and 220 ± 100 nm).

In addition, 170 ± 80 nm salbutamol sulfate-loaded nanoparticles are produced using the same technique. However, the nanoparticles size is not varied for the salbutamol sulfate due to the low drug loading obtainable for nanoparticles sizes smaller than 170 ± 80 nm. The low drug loading is attributed to the high aqueous solubility of the salbutamol sulfate, such that the drug quickly diffuses out from the polymer to the aqueous phase during the nanoprecipitation process.

In the present work, the reported amount of drug released is based on three independent UV–vis measurements for both the aspirin and salbutamol sulfate. The experimental uncertainty in the values of the drug release rate is approximately 3%, which is based on the average of the uncertainty values at the seven sampling times (i.e. 1/2, 1, 2, 3, 4, 7, 24 h). Importantly, the results of the drug release study indicate that the free-drug particles are completely dissolved within 4 h (see Figs. 4 and 5), which

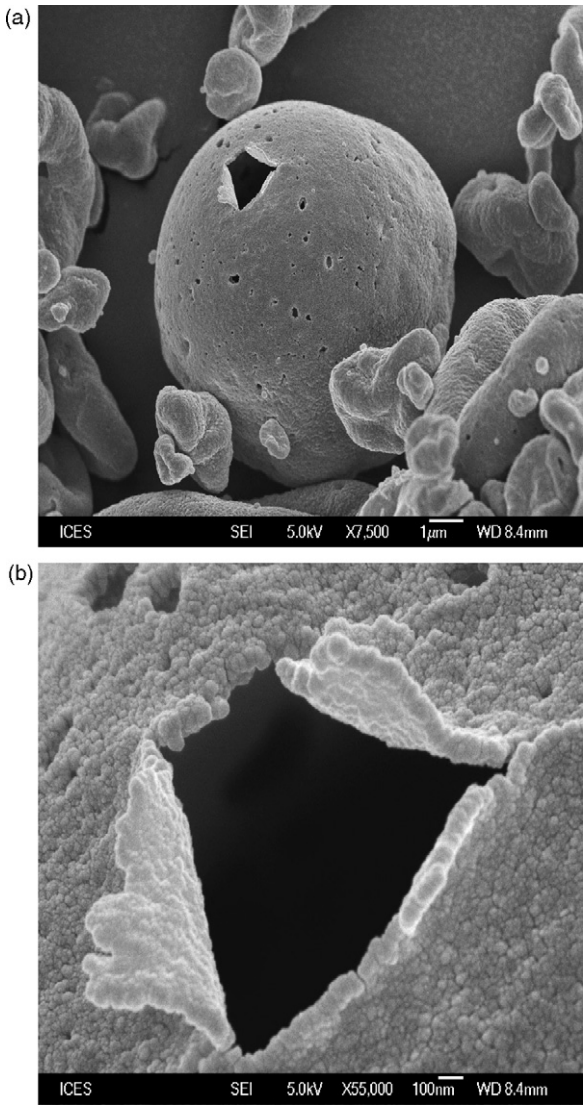

Fig. 3. (a) A closer look at the LHP of the 70 ± 30 nm without loaded drug spray-dried at 1.9% (w/w). (b) A close-up view of the nanoparticulate aggregates on the surface of the 70 ± 30 nm LHP.

signifies the absence of drug absorption onto the dialysis bag membrane. Furthermore, a majority of the NP and LHP systems investigated are capable of releasing about 90% of the loaded drug within a 24-h period (see Table 1).

Fig. 4 shows the results of the aspirin release profile as a function of the nanoparticles size, where each size exhibits a different drug loading capacity. The drug loading of the aspirin-loaded NP increases from about 2.0–5.0% for the 50 ± 20 and 70 ± 30 nm NP to about 9.0% for the 120 ± 40 nm NP. Correspondingly, the drug loading of the aspirin-loaded LHP increases from 1.5–3.5% for the 50 ± 20 and 70 ± 30 nm LHP to about 9.0% for the 120 ± 40 nm LHP. The lower drug loadings of the 50 ± 20 and 70 ± 30 nm LHP, compared to their NP counterparts, are due to the additional drug lost during the spray drying process.

The results indicate that the aspirin release profiles of both the NP and LHP at NP drug loadings of 9.0 and 5.0% (see

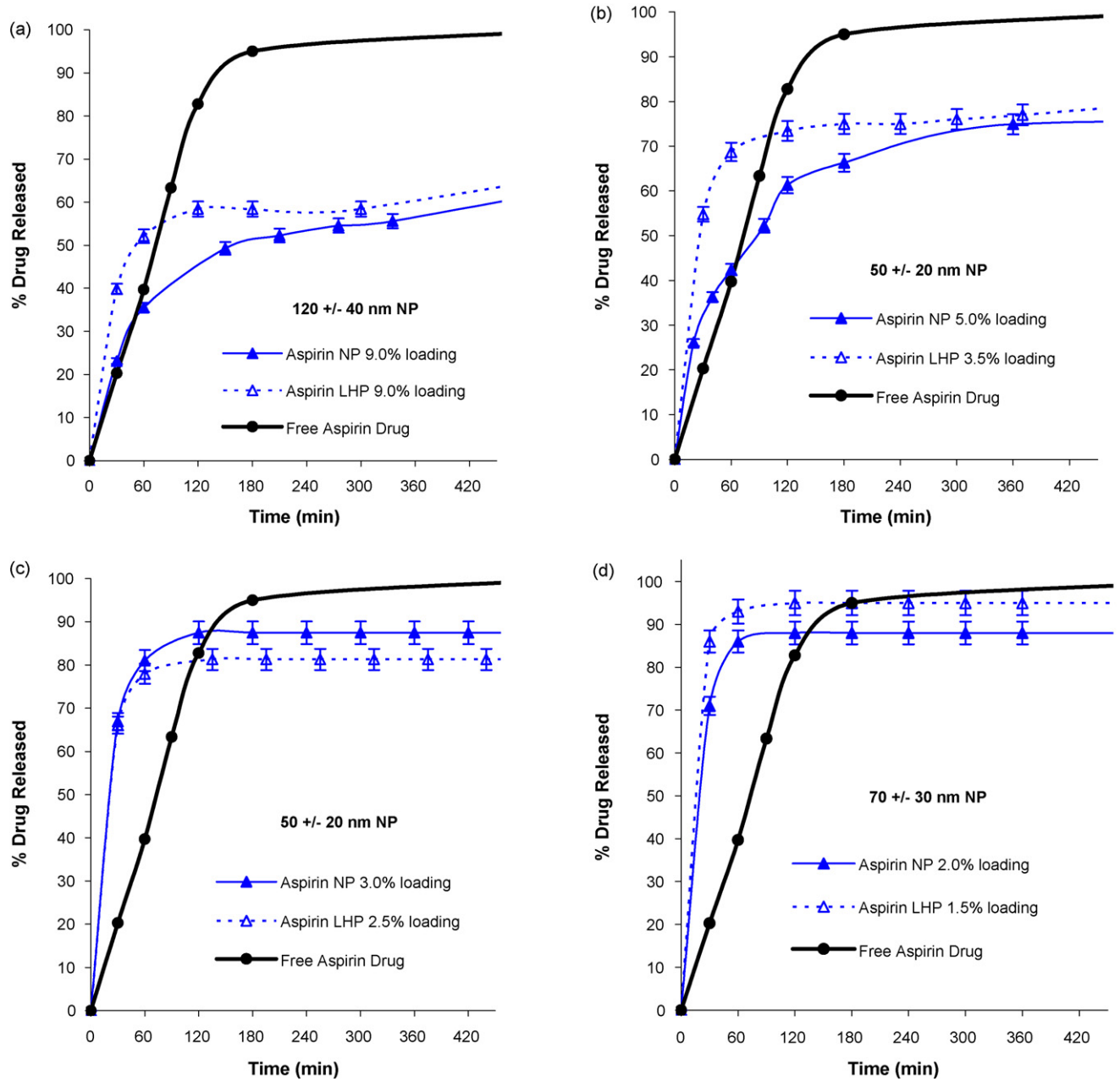

Fig. 4. (a) Aspirin drug release profile of the 120 ± 40 nm LHP at 9.0% NP drug loading. (b) Aspirin drug release profile of the 50 ± 20 nm LHP at 5.0% NP drug loading. (c) Aspirin drug release profile of the 50 ± 20 nm LHP at 3.0% NP drug loading. (d) Aspirin drug release profile of the 70 ± 30 nm LHP at 2.0% NP drug loading.

Fig. 4a and b, respectively) exhibit a biphasic type of behavior, which consists of a burst release phase that is followed by a slower steady release phase. In contrast, the drug release profiles of the NP and LHP at NP drug loadings of 3.0 and 2.0% (see Fig. 4c and d, respectively) exhibit a monophasic behavior of a burst release phase in which close to 90% of the drug is released in less than 1 h. To be exact, the percentage amount of the drug released after 1 h is 52, 69, 78 and 93% for the LHP with 9.0, 3.5, 2.5, and 1.5% drug loading, respectively. Therefore, the results signify an increase in the degree of the burst release rate for both the NP and LHP with the decrease in the drug loading, which is associated with the decrease in the nanoparticles size. Accordingly, the NP and LHP exhibit an almost identical monophasic-burst release profile at low drug loading.

In contrast to the aspirin, where the biphasic release profile is only observed for NP drug loading above 5.0%, the salbutamol sulfate drug release profiles exhibit a biphasic type of behavior for both the NP and LHP at a lower NP drug loading of 2.0% (see Fig. 5). The difference in the release profiles of the two drugs at NP drug loading of 2.0% results from the combined effects that stem from the variations in (1) the size of the salbutamol sulfate-loaded NP (170 ± 80 nm) and the aspirin-loaded NP (70 ± 30 nm), (2) the morphology of their corresponding

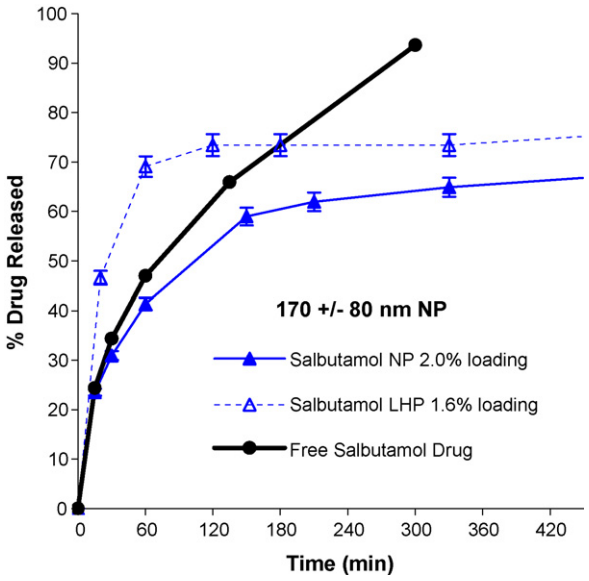

Fig. 5. Salbutamol sulfate drug release profile of the 170 ± 80 nm LHP at 2.0% NP drug loading.

LHP, and/or (3) the physicochemical properties of the drugs themselves.

3.2.2. Different nanoparticles size, constant drug loading

In Section 3.2.1, the dependence of the drug release rate on the nanoparticles size is directly related to the drug loading, as the variation in the nanoparticles size leads to a variation in the drug loading. To complement the aforementioned results, the effect of the nanoparticles size on the aspirin drug release rate is isolated by conducting a drug release study of two NP/LHP systems of two different nanoparticles sizes (i.e. 120 ± 40 and 220 ± 100 nm), which exhibit approximately similar drug loadings (i.e. 9.0 and 10.0%, respectively).

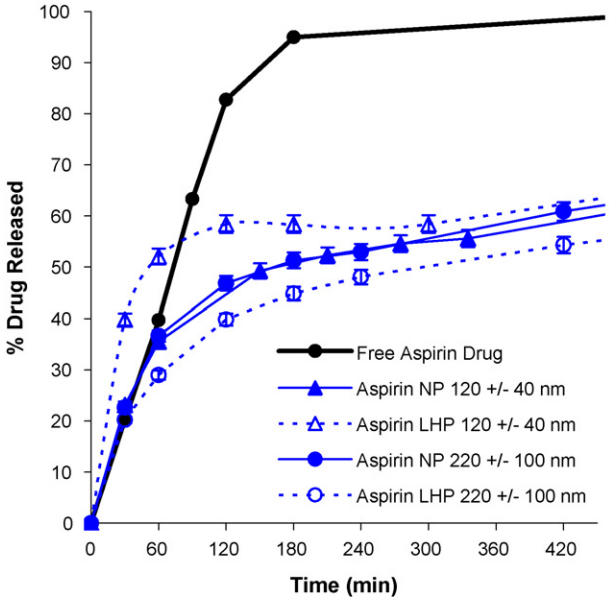

Fig. 6. Aspirin drug release profile of the 120 ± 40 and 220 ± 100 nm LHP at 9.0% and 10.0% drug loading, respectively.

The results in Fig. 6 indicate that the drug release rate of the NP is not affected by the increase in the nanoparticles size from 120 ± 40 to 220 ± 100 nm. On the other hand, the drug release rate of the 220 ± 100 nm LHP exhibits a significantly slower release compared to that of the 120 ± 40 nm LHP. It takes approximately 7 h for the 220 ± 100 nm LHP to dissolve 60% of the drug, whereas it only takes less than 3 h for the 120 ± 40 nm LHP to do likewise. Over a 24-h period, only about 80% of the drug is released from the 220 ± 100 nm LHP, compared to a 95% release for the 120 ± 40 nm LHP. In addition, for the 220 ± 100 nm LHP, the drug is released at a slower rate than that of the 220 ± 100 nm NP, which is not observed previously with the other nanoparticles sizes (i.e. 50 ± 20, 70 ± 30, and 120 ± 40 nm). Therefore, the variation in the drug release rate of these two LHP systems must be caused by factors other than the nanoparticles size, because their release rates at the NP level are found not to be affected by the nanoparticles size difference (see Section 4.1.2 below).

3.3. Drug release rate as a function of the phospholipids concentration

The inclusion of the phospholipids in the LHP formulation was found to significantly influence the resulting morphology (i.e. size and degree of hollowness) of the spray-dried LHP in Hadinoto et al. (2007). Most importantly, varying the phospholipids concentration led to a variation in the degree of hollowness, without affecting the fine particle production. In other words, the presence of the phospholipids did not significantly influence the resulting LHP particle size distribution. Therefore, varying the phospholipids concentration, instead of the nanoparticles concentration, was concluded to be the preferred method for controlling the degree of hollowness of the LHP. Recognizing the significant effects of the phospholipids inclusion on the LHP morphology, and the importance of the LHP morphology on the drug release rate (see Section 4.1.2 below), the effect of the phospholipids concentration on the LHP drug release rate is investigated.

The studies are conducted for both the aspirin-loaded LHP (120 ± 40 and 220 ± 100 nm) and salbutamol sulfate-loaded LHP (170 ± 80 nm) (see Table 2). The phospholipids are dissolved in 5 mL ethanol and added to 100 mL nanoparticulate suspension prior to the spray drying process. Fig. 7 shows that the phospholipids inclusion (up to 27% of the total solid content) does not affect the initial burst release rate of the aspirin (<30 min) for the 120 ± 40 nm LHP. However, adding the phospholipids leads to an increase in the amount of drug released after 2 h from about 60%, in the absence of the phospholipids, to about 80% at 27% phospholipids concentration.

Similar to the 120 ± 40 nm LHP, Fig. 8a indicates that the phospholipids inclusion at varying concentration does not affect the initial burst release rate of the aspirin in the 220 ± 100 nm LHP. In contrast to the 120 ± 40 nm LHP, however, the amount of drug released after 2 h remains constant at about 50% for all the phospholipids concentrations investigated. The effect of increasing the phospholipids concentration on the drug release profile of the 220 ± 100 nm LHP starts to intensify only after

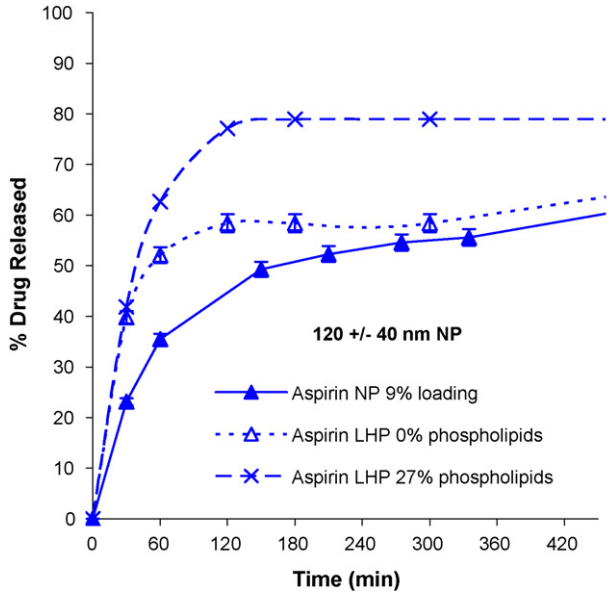

Fig. 7. Aspirin drug release profile of the 120 ± 40 nm LHP at 9.0% NP drug loading as a function of the phospholipids concentration.

8 h. Over a 24-h period, Fig. 8b shows that the amount of drug released decreases from about 80% in the absence of the phospholipids, to about 65% at 24% phospholipids concentration. Again, the results are in contrast to the results of the 120 ± 40 nm LHP, where an increase in the amount of drug released is observed with increasing phospholipids concentration. Furthermore, despite the presence of the phospholipids at the LHP surface, the 220 ± 100 nm LHP yet exhibit a slower release rate than that of the 220 ± 100 nm NP (see Fig. 8a), which has been observed previously in the absence of the phospholipids (see Section 3.2.2).

In addition, the effect of the phospholipids inclusion on the release of salbutamol sulfate from the 170 ± 80 nm LHP is investigated. In contrast to the results for the aspirin, Fig. 9 indicates that the phospholipids inclusion affects the initial burst release rate of the salbutamol sulfate, where the burst release rate is reduced with increasing phospholipids concentration. As a result, the amount of drug released after 2 h is also reduced with increasing phospholipids concentration, from about 75% in the absence of the phospholipids, to about 60% at 33% phospholipids concentration.

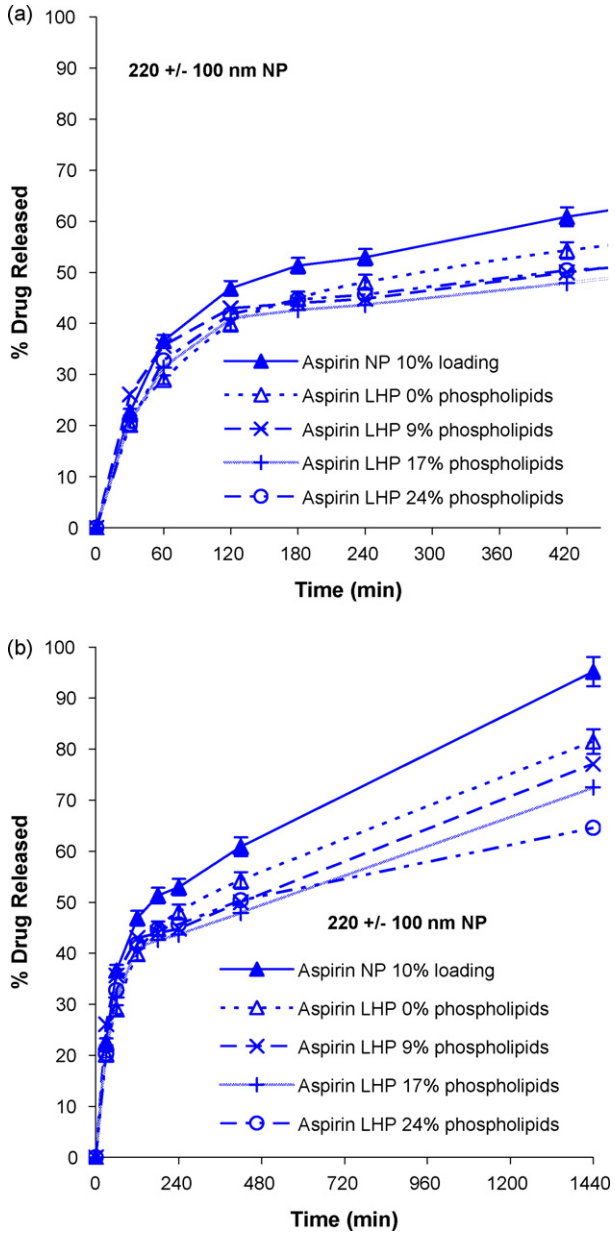

Fig. 8. Aspirin drug release profile of the 220 ± 100 nm LHP at 10.0% NP drug loading as a function of the phospholipids concentration: (a) 7-h release profile; (b) 24-h release profile.

4. Discussion

4.1. Effect of the nanoparticles size on drug release rate

4.1.1. Effect of the nanoparticles size, different drug loading

The burst release phase, which is commonly observed in the release study of small-molecules therapeutics (Cohen et al., 1991), is attributed to the rapid release of the surface-adsorbed drug, which is readily accessible by the buffer medium. In the preparation of the polymer nanoparticles using the nanoprecipitation technique, the accumulation of the drug at the nanoparticles surface is caused by the polymer nanoprecipitation process that occurs earlier than the drug precipitation (Leo et al., 2004), which results in a majority of the drug precipitates on the nanoparticles surface. Following the burst release of the surface-adsorbed drug, a slower steady release of the drug entrapped within the polymer matrix takes place, hence leads to the overall biphasic drug release profile reported in Section 3.2.1.

Furthermore, the results in Fig. 4 also indicate that the initial release rate of the free-drug particles of aspirin (micronized particle ≈100 μm; Sigma–Aldrich) is slower than that of the drug encapsulated in the polymer nanoparticles (at both NP and LHP levels), particularly for the smaller size nanoparticles. The higher initial release rate of the encapsulated nanoparticulate drug is due to the higher dissolution rate of the nanoparticles compared

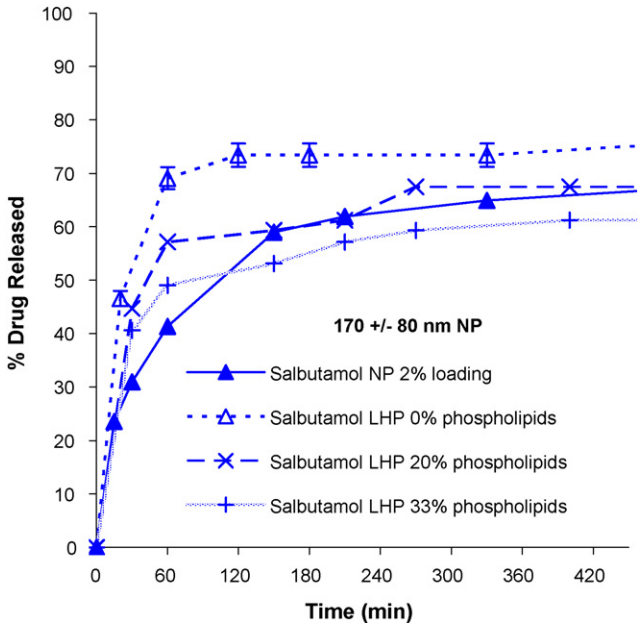

Fig. 9. Salbutamol sulfate drug release profile of the 170 ± 80 nm LHP at 2.0% NP drug loading as a function of the phospholipids concentration.

to their micron-size particle counterparts. On the other hand, Fig. 5 indicates that the initial release rate of the micronized free-drug particles of salbutamol sulfate is comparable to that of the 170 ± 80 nm polymer nanoparticles, which is attributed to the very high aqueous solubility of the salbutamol sulfate.

Notably, the release rate of the polymer nanoparticles at NP drug loading of 9.0% slows down significantly after the initial burst release phase that lasts for about 30 min (see Fig. 4a). The slowing down of the release rate is not observed in the free-drug particles, or in the polymer nanoparticles at a lower drug loading. At NP drug loading of 9.0%, the slower aspirin drug release rate, after the initial burst release phase, indicates that an increased fraction of the drug becomes entrapped within the polymer matrix (as in not completely adsorbed on the nanoparticles surface) with increasing drug loading. As the drug becomes physically or molecularly dispersed within the polymer matrix, the drug release mechanism is now governed by a combination of polymer breakdown (i.e. matrix erosion) and diffusion out of the polymer matrix.

The dependence of the drug release mechanism upon the matrix erosion and diffusion has been found to lead to a slower drug release rate (Erden and Celebi, 1996; Caliceti et al., 2000). Accordingly, the drug release profiles of the NP and LHP presented in Fig. 4a exhibit a slower release rate compared to the release profiles at a lower drug loading (see Fig. 4b–d). At 9.0% drug loading, only about 60% of the drug is released after 7 and 2 h for the NP and LHP, respectively. On the other hand, at 3.0% drug loading, 80% of the drug is released within 2 h from both the NP and LHP. Correspondingly, it takes 24 h to dissolve 90% of the drug at 9.0% drug loading, compared to just about 3 h at 3.0% drug loading (see Table 1). Moreover, the average molecular weight (M_w) of the polymer nanoparticles determined by the GPC is shown to decrease from 32,000 for the fresh LHP to about 20,000 after 24-h immersion in the drug release medium. The molecular weight loss corresponds with the gradual bulk erosion of the polymer matrix into its chemical constituents.

More importantly, the results in Fig. 4 indicate that the aspirin drug is released more rapidly from the LHP compared to that from the NP. A similar observation is made for the salbutamol sulfate-loaded NP and LHP (see Fig. 5). The higher drug release rate of the spray-dried LHP is postulated due to the nanoparticles being exposed to a high temperature, which exceeds the glass transition temperature (T_g) of the polymer. The DSC analysis (HyperDSC, Perkin-Elmer, USA) reveals that the glass transition temperature of the polymer is ~65 °C. The adopted scanning temperature range in the DSC analysis is from 25 to 300 °C at a heating rate of 10 °C/min. The outlet temperature in the spray drying chamber is approximately 60 ± 5 °C, hence closely approaches the T_g value of the polymer. The exposure to the high temperature close to their T_g value leads to the nanoparticles being softened and deformed into their rubbery or less stable state, which alters the dispersion of the drug in the polymer nanoparticles. The subsequent change in the solid-state of the polymer nanoparticles influences the drug release rate, where drugs have been found to be released more readily from rubbery-state polymeric delivery systems (Fan and Singh, 1989; Siepmann et al., 2004).

In a summary, for the same initial amount of drug used in the formulation, an increase in the drug loading and drug entrapment efficiency of the nanoparticles is observed with increasing nanoparticles size. The increased drug loading subsequently leads to a biphasic drug release profile for both the NP and LHP (in place of the monophasic-burst release profile), which is attributed to a larger fraction of the drug becomes entrapped within the polymer matrix at high drug loading.

4.1.2. Effect of the nanoparticles size, constant drug loading

The results presented in Section 3.2.2 lead to a conclusion that the slower drug release rate of the 220 ± 100 nm LHP (compared to that of the 120 ± 40 nm LHP) is attributed more to the resulting morphology of the LHP, rather than to the NP size. One feature that best characterizes the LHP morphology is the degree of hollowness, which is inversely proportional to the ratio of the effective density to the true density of the particles (ρ_e/ρ_{true}). The density ratio was quantified in Hadinoto et al. (2007) by measuring the value of $\psi^{dia} = (d_a/d_g)^2$. The diameter ratio measurement was shown to be the more accurate technique in quantifying the degree of hollowness, compared to the conventional technique of tap density measurement.

In the present work, the diameter ratio measurement indicates that the ψ^{dia} value of the 220 ± 100 nm LHP is about 0.14, whereas that of the 120 ± 40 nm LHP is significantly lower at 0.05, with 10% experimental uncertainties. Therefore, the 220 ± 100 nm LHP, which are spray-dried at 2.3% (w/w) nanoparticles concentration, are significantly less hollow compared to their 120 ± 40 nm LHP counterparts, which are spray-dried at 1.4% (w/w) nanoparticles concentration (see Table 1). The results are consistent with the findings of Hadinoto

et al. (2006), which concluded that the degree of hollowness of the acrylic polymer LHP decreased with increasing spray drying nanoparticles concentration. The decrease in the degree of hollowness of the LHP with increasing nanoparticles concentration is caused by an increased production of nearly solid fine particles ($\leq$5 μm), which exhibit a thicker shell. As a result, a decrease in the degree of hollowness with increasing nanoparticles concentration is often accompanied by a shift in the LHP particle size distribution toward a smaller mean size.

Because the degree of hollowness of the 220 ± 100 nm LHP is lower than that of the 120 ± 40 nm LHP, the relative shell thickness (with respect to the particle radius) of the 220 ± 100 nm LHP is larger. The larger relative shell thickness results in the shell becoming less susceptible to physical deformation due to external forces (Sugiyama et al., 2006). Accordingly, the nanoparticulate aggregates in the 220 ± 100 nm LHP exhibit a higher resistance to re-dispersion into their primary nanoparticles upon dissolution. As a result, the 220 ± 100 nm LHP are more difficult to be re-dispersed into their primary NP, compared to the 120 ± 40 nm LHP, which are readily re-dispersed due to their thinner shell. Consequently, the drug release rate of the 220 ± 100 nm LHP, where the drug is released from larger size aggregates, is significantly slower than that of the 120 ± 40 nm LHP.

4.2. Effect of the phospholipids concentration on drug release rate

The wide variation in the drug release results as a function of the phospholipids concentration presented in Section 3.3 indicates that the effect of the phospholipids inclusion on the drug release rate varies for different types of drug. Importantly, the variation in the effect of the phospholipids concentration on the aspirin drug release rate, between the 120 ± 40 nm LHP ($\psi^{dia} = 0.05$) and the 220 ± 100 nm LHP ($\psi^{dia} = 0.14$), re-emphasize the significant role of the LHP morphology on the drug release rate. Hence, the slower release rate of the 220 ± 100 nm LHP compared to their corresponding NP is also thought due to the large relative shell thickness of the 220 ± 100 nm LHP (see Section 4.1.2), despite the presence of the phospholipids.

For the 120 ± 40 nm LHP, the increase in the amount of drug released with the phospholipids inclusion is postulated due to the accumulation of the amphiphilic phospholipids at the LHP surface, which has been verified by X-ray photoelectron spectroscopy (XPS) in Hadinoto et al. (2007). The presence of the phospholipids at the surface leads to an increase in the surface hydrophilicity of the hydrophobic polymer. As a result, water uptake by the polymer is increased leading to an enhanced rate of the bulk polymer erosion, which subsequently leads to a faster drug release rate (Cohen et al., 1991).

Another explanation for the increase in the drug release rate is the fact that the degree of hollowness of acrylic polymer LHP increased with increasing phospholipids concentration in Hadinoto et al. (2007). The reported ψ^{dia} value of the LHP decreased from 0.13 to 0.05, when the phospholipids concentration was increased from 0% to 33% of the total solid content. Accordingly, the 120 ± 40 nm LHP exhibit a thinner shell at 27% phospholipids concentration than that at 0% concentration. As the nanoparticulate aggregates in the thinner shell are more readily re-dispersed into the primary NP, the 120 ± 40 nm LHP formulated at a high phospholipids concentration exhibit a larger amount of the drug released.

5. Conclusion

The results of our study demonstrate that the drug loading capacity of the LHP formulated in the present work is only slightly lower, if not similar, to that of the primary NP constituting the LHP. The closely similar drug loading values between the NP and LHP indicate that a majority of the drug loaded during the nanoprecipitation step is preserved throughout the spray drying process. Importantly, the LHP drug release pattern behaves according to that of the NP, even though the rate at which the drug is released is faster for the LHP, which is due to the change in the solid-state of the polymer after spray drying. These two positive attributes of the LHP make them highly suitable to serve as the carrier particles in pulmonary delivery of nanoparticulate drugs.

In addition, the LHP drug release rate is found to be highly dependent on the resulting morphology of the LHP (i.e. size and degree of hollowness). The drug release rate is also dependent, though to a lesser degree, on the size of the primary NP. In other words, for two LHP systems of two distinct NP sizes, the drug release rates of the two LHP systems can vary, even though their release rates are similar at the NP level, if they exhibit a different degree of hollowness at the LHP level. LHP with less degree of hollowness (i.e. thicker shell) exhibit a significantly slower drug release rate, as the nanoparticulate aggregates in a thicker shell exhibit a higher resistance to re-dispersion into the primary NP upon dissolution. Furthermore, increasing the NP size leads to an increase in the drug loading capacity of the NP. The increased drug loading capacity subsequently leads to a gradual shift from the monophasic-burst release profile to the more desirable slower-biphasic release profile. Lastly, the effect of the phospholipids inclusion on the LHP drug release rate is governed not only by the drug physicochemical properties, but also by the resulting LHP morphology.

Acknowledgements

The authors would like to thank Chew Meizeng for her contribution in the drug release experiments, and A*STAR (Agency for Science, Technology and Research) of Singapore, Grant ICES/05-122001, for funding this work.

Appendix A. Test of statistical significance

A.1. Methods

1. For the test of statistical significance, n number independent experimental measurements of samples 1 and 2 are conducted to form n number independent replicates. The parameter of interest is the percentage amount of drug released, which

is determined by measuring the UV–vis absorbance of the samples.

2. In the present work, $n_1 = n_2 = 3$, hence three aliquots each of samples 1 and 2 are drawn and analyzed using the UV–vis spectrometer. The mean (x_1, x_2) and standard deviation (s_1, s_2) of the samples, based on the three independent replicates of the UV–vis absorbance values, are subsequently determined (Montgomery and Runger, 1999):

$$t_{\text{calc}} = \frac{x_1 - x_2}{\sqrt{(s_1^2/n_1) + (s_2^2/n_2)}} \quad \text{(A.1)}$$

$$\text{D.O.F} = \frac{((s_1^2/n_1) + (s_2^2/n_2))^2}{((s_1^2/n_1)^2/(n_1+1)) + ((s_2^2/n_2)^2/(n_2+1))} - 2 \quad \text{(A.2)}$$

3. The t-test is conducted to determine the statistical significance of the effects of (a) the nanoparticles size, different drug loading (Section 3.2.1), (b) the nanoparticles size, constant drug loading (Section 3.2.2), and (c) the phospholipids inclusion (Section 3.3) on the drug release rates of both the NP and LHP. For (a) and (b), the analysis is conducted for the 1-h release data, whereas for (c), the analysis is conducted for the 1-, 7- and 24-h release data (see Table A.1).
4. For the effect of the nanoparticles size at different drug loading, the t-test analysis is conducted using the 120 ± 40 nm NP/LHP and the 70 ± 30 nm NP/LHP as the representative samples. The analysis is conducted at the highest (subscript 1) and lowest (subscript 2) drug loadings (see Table A.1). For the effect of the nanoparticles size at a constant drug loading, the t-test analysis is conducted using the 120 ± 40 nm NP/LHP at 9.0% loading and the 220 ± 100 nm NP/LHP at 10.0% loading as the representative samples. For the effect of the phospholipids inclusion, the analysis is conducted using the aspirin-loaded 220 ± 100 nm LHP and the salbutamol sulfate-loaded 170 ± 80 nm LHP as the representative samples, where the test is conducted at the highest (subscript 2) and lowest (subscript 1) phospholipids concentrations.
5. The hypothesis to be tested is H1: $\mu_1 - \mu_2 = 0$, which indicates that the population means of samples 1 and 2 are equal, such that the difference in the sample means x_1 and x_2 is statistically insignificant, as it is due to a random occurrence.
6. For $\alpha = 0.05$, the hypothesis H1 is rejected when $t_{\text{calc}} > t_{\alpha/2,\text{D.O.F.}}$ or when $t_{\text{calc}} < -t_{\alpha/2,\text{D.O.F.}}$. If the hypothesis H1 is rejected, it indicates that there is a strong statistical evidence that the reported trends in the drug release rate as a function of the nanoparticles size and phospholipids concentration are statistically significant, and not due to a random occurrence.

A.2. Results

A.2.1. The effect of the nanoparticles size, different drug loading

The results of the t-test analysis for $\alpha = 0.05$ presented in Table A.1 show that $t_{\text{calc}} < -t_{\alpha/2,\text{D.O.F.}}$ for both the NP and LHP at two different drug loadings. Therefore, the reported trend in the drug release rate of the NP and LHP as a function of the drug loading in Section 3.2.1 is statistically significant, and not due to a random occurrence.

A.2.2. The effect of the nanoparticles size, constant drug loading

The t_{calc} result indicates that $-t_{\alpha/2,\text{D.O.F.}} < t_{\text{calc}} < t_{\alpha/2,\text{D.O.F.}}$ for the NP. Hence, it reaffirms the conclusion reported in Section 3.2.2 that the drug release rates of the 120 ± 40 and 220 ± 100 nm NP are identical at the NP level. On the contrary, the t_{calc} result indicates that $t_{\text{calc}} > t_{\alpha/2,\text{D.O.F.}}$ for the LHP, which reiterates the conclusion that the difference in the drug release rates between the 120 ± 40 nm LHP and the 220 ± 100 nm LHP is indeed due to the difference in their resulting LHP morphology, and not due to a random occurrence.

Table A.1

Sample	Data #1	Drug loading (%)	x_1	s_1	Data #2	Drug loading (%)	x_2	s_2	D.O.F.	$\alpha = 0.05 t_{\alpha/2,\text{D.O.F.}}$	t_{calc}
Section 3.2.1											
NP 1-h release	120 ± 40 nm	9.0	35.5	2.1	70 ± 30 nm	2.0	86.0	5.2	3	3.182	−15.669
LHP 1-h release	120 ± 40 nm	9.0	52.2	3.1	70 ± 30 nm	1.5	93.0	5.6	4	2.776	−11.076
Section 3.2.2											
NP 1-h release	120 ± 40 nm	9.0	35.5	2.1	220 ± 100 nm	10.0	36.6	2.2	6	2.447	−0.623
LHP 1-h release	120 ± 40 nm	9.0	52.2	3.1	220 ± 100 nm	10.0	28.9	1.7	4	2.776	11.241
Section 3.3											
LHP 1-h release Phospholipids (%)	220 ± 100 nm 9	10.0	35.7	2.1	220 ± 100 nm 24	10.0	32.8	2.0	6	2.447	1.727
LHP 24-h release Phospholipids (%)	220 ± 100 nm 9	10.0	77.1	0.8	220 ± 100 nm 24	10.0	64.6	0.6	6	2.447	21.524
LHP 1-h release Phospholipids (%)	170 ± 80 nm 20	1.6	57.2	1.7	170 ± 80 nm 33	1.6	49.1	1.5	6	2.447	6.204
LHP 7-h release Phospholipids (%)	170 ± 80 nm 20	1.6	67.5	2.0	170 ± 80 nm 33	1.6	61.2	1.8	6	2.447	3.992

A.2.3. The effect of the phospholipids inclusion

Aspirin. The t_{calc} result for the 220 ± 100 nm LHP at the 1-h release point indicates that $-t_{\alpha/2,D.O.F.} < t_{calc} < t_{\alpha/2,D.O.F.}$. Hence, it reaffirms the conclusion reported in Section 3.3 that the phospholipids inclusion does not affect the initial burst release rate of the aspirin. On the other hand, the t_{calc} result at the 24-h release point indicates that $t_{calc} > t_{\alpha/2,D.O.F.}$, which signifies that the reported effect of the phospholipids inclusion on the long-term release of the aspirin is statistically significant.

Salbutamol sulfate. The t_{calc} results for the 170 ± 80 nm LHP indicate that $t_{calc} > t_{\alpha/2,D.O.F}$ for both the 1- and 7-h release points. Therefore, the reported trend in the drug release profile of salbutamol sulfate as a function of the phospholipids concentration is statistically significant, and not due to a random occurrence.

References

Ahsan, F., Rivas, I.P., Khan, M.A., Suarez-Torres, A.I., 2002. Targeting to macrophages: role of physicochemical properties of particulate carriers-liposomes and microspheres on the phagocytosis by macrophages. J. Controlled Release 79, 29–40.

Caliceti, P., Veronese, F.M., Lora, S., 2000. Polyphosphazene microspheres for insulin delivery. Int. J. Pharm. 211, 57–65.

Cohen, S., Yoshioka, T., Lucarelli, M., Hwang, L.H., Langer, R., 1991. Controlled delivery systems for protein based on poly(lactic/glycolic acid) microspheres. Pharm. Res. 8, 713–720.

Dailey, L.A., Kleeman, E., Wittmar, M., Gessler, T., Schmehl, T., Roberts, C., Seeger, W., Kissel, T., 2003. Surfactant-free, biodegradable nanoparticles for aerosol therapy based on the branched polyesters. DEAPA-PVAL-g-PLGA. Pharm. Res. 20, 2011–2020.

Edwards, D.A., Hanes, J., Caponetti, G., Hrkach, J., Ben-Jebria, A., Eskew, M., Mintzes, J., Deaver, D., Lotan, N., Langer, R., 1997. Large porous particles for pulmonary drug delivery. Science 276, 1868–1871.

Erden, N., Celebi, N., 1996. Factors influencing release of salbutamol sulphate from poly(lactide-co-glycolide) microspheres prepared by water-in-oil-in-water emulsion technique. Int. J. Pharm. 137, 57–66.

Fan, L.T., Singh, S.K., 1989. Controlled Release: A Quantitative Treatment. Springer-Verlag, Berlin.

Guo, Q.Y., Chan, L.W., Heng, P.W.S., 2005. Investigation of the release of aspirin from spray-congealed micro-pellets. J. Microencapsul. 22, 245–251.

Hadinoto, K., Phanapavudhikul, P., Zhu, K., Tan, R.B.H., 2006. Novel formulation of large hollow nanoparticles aggregates as potential carriers in inhaled delivery of nanoparticulate drugs. Ind. Eng. Chem. Res. 45, 3697–3706.

Hadinoto, K., Phanapavudhikul, P., Zhu, K., Tan, R.B.H., 2007. Dry powder aerosol delivery of large hollow nanoparticulate aggregates as prospective carriers of nanoparticulate drugs: effects of phospholipids. Int. J. Pharm. 333, 187–198.

Hoet, P., Bruske-Hohlfeld, I., Salata, O.V., 2004. Nanoparticles—known and unknown health risks. J. Nanobiotechnol. 2, doi:10.1186/1477-3155-2-12.

Leo, E., Brina, B., Forni, F., Vandelli, M.A., 2004. In vitro evaluation of PLA nanoparticles containing a lipophilic drug in water-soluble or insoluble form. Int. J. Pharm. 278, 133–141.

Makino, K., Yamamoto, N., Higuchi, K., Harada, N., Ohshima, H., Terada, H., 2003. Phagocytic uptake of polystyrene microspheres by alveolar macrophages: effects of the size and surface properties of the microspheres. Colloid Surf. B 27, 33–39.

Montgomery, D.C., Runger, G.C., 1999. Applied Statistics and Probability for Engineers. John Wiley and Sons, New York, pp. 388–394.

Phanapavudhikul, P., Waters, J.A., Ortiz, E.S., 2002. Para-magnetic composite microparticles as heavy metal ion-exchangers. Eur. Cells Mater. 3, 118–121.

Sanchez, A., Vila-Jato, J.L., Alonso, M., 1993. Development of biodegradable microspheres and nanospheres for the controlled release of cyclosporin A. Int. J. Pharm. 99, 263–273.

Siepmann, J., Faisant, N., Akiki, J., Richard, J., Benoit, J.P., 2004. Effect of the size of biodegradable microparticles on drug release: experiment and theory. J. Controlled Release 96, 123–124.

Soppimath, K.S., Aminabhavi, T.M., Kulkarni, A.R., Rudziski, W.E., 2001. Biodegradable polymeric nanoparticles as drug delivery devices. J. Controlled Release 70, 1–20.

Stanek, L.G., Heilmann, S.M., Gleason, W.B., 2006. Preparation of monodisperse PMMA microspheres using 2-vinyl-4,4′-dimethyllazlactone as a particle stabilizer. Colloid Polym. Sci. 284, 586–595.

Sugiyama, Y., Larsen, R.J., Kim, J.W., Weitz, D.A., 2006. Buckling and crumpling of drying droplets of colloid-polymer suspensions. Langmuir 22, 6024–6030.

Tao, S.L., Lubeley, M.W., Desai, T.A., 2003. Bioadhesive poly(methyl methacrylates) microdevices for controlled drug delivery. J. Controlled Release 88, 215–228.

Tapolsky, G., Li, Y., Jiao, Y., 2005. Magnetically targetable particles comprising magnetic components and biocompatible polymers for site-specific delivery of biologically active agents. World Patent No. WO 2005/025508 A2.

Torrado, S., Cadorniga, R., Torrado, J.J., 1996. Effect of drug release rate on bioavailability of different aspirin tables. Int. J. Pharm. 133, 65–70.

Tsapis, N., Bennet, D., Jackson, B., Weitz, D.A., Edwards, D.A., 2002. Trojan particles: large porous carriers of nanoparticles for drug delivery. Proc. Natl. Acad. Sci. USA 99, 12001–12005.